Published September 24, 2010, doi:10.4049/jimmunol.1001734

The Protein Tyrosine Kinase Tec Regulates a CD44^{high} CD62L^{-} Th17 Subset

Nicole Boucheron,* Omar Sharif,[†,‡] Alexandra Schebesta,* Andrew Croxford,[§] Julia Raberger,*[,1] Uwe Schmidt,*[,2] Benjamin Vigl,*[,3] Jan Bauer,[¶] Rashmi Bankoti,[‖,4] Hans Lassmann,[¶] Michelle M. Epstein,[‖] Sylvia Knapp,[†,‡] Ari Waisman,[§] and Wilfried Ellmeier*

The generation of Th17 cells has to be tightly controlled during an immune response. In this study, we report an increase in a CD44^{high} CD62L^{-} Th17 subset in mice deficient for the protein tyrosine kinase Tec. CD44^{high}CD62L^{-} *Tec*$^{-/-}$ CD4^{+} T cells produced enhanced IL-17 upon activation, showed increased expression levels of IL-23R and RORγt, and IL-23–mediated expansion of *Tec*$^{-/-}$ CD4^{+} T cells led to an increased production of IL-17. *Tec*$^{-/-}$ mice immunized with heat-killed *Streptococcus pneumoniae* displayed increased IL-17 expression levels in the lung postinfection with *S. pneumoniae*, and this correlated with enhanced pneumococcal clearance and reduced lung inflammation compared with *Tec*$^{+/+}$ mice. Moreover, naive *Tec*$^{-/-}$ OT-II CD4^{+} T cells produced higher levels of IL-17 when cultured with OVA peptide-loaded bone marrow-derived dendritic cells that have been previously activated with heat-killed *S. pneumoniae*. Taken together, our data indicated a critical role for Tec in T cell-intrinsic signaling pathways that regulate the in vivo generation of CD44^{high}CD62L^{-} effector/memory Th17 populations. *The Journal of Immunology*, 2010, 185: 000–000.

Members of the Tec kinase family (Tec, Btk, Itk, Rlk, and Bmx) play an important role during lymphocyte development and activation, and mutations in Tec family kinases are linked with immunodeficiencies in humans and mice (1, 2). Three members of the Tec kinase family are expressed in T cells: Tec, Itk, and Rlk. *Itk*$^{-/-}$ mice have defects in T cell development, affecting in particular conventional T cells, thus leading to increased numbers of CD4^{+} and CD8^{+} T cells with a CD44^{high}CD62L^{-} effector/memory phenotype that rapidly secrete high levels of effector cytokines such as IFN-γ after PMA/ionomycin stimulation and thus were described as innate-like T cells. Moreover, TCR-mediated activation and proliferation of naive T cells as well as their polarization into Th2 effector T cells are impaired in the absence of Itk. Additionally, Itk is also important in the activation of β_1 integrins and the regulation of the actin cytoskeleton upon activation. Several studies implied a role for Rlk in Th1 cell polarization, although *Rlk*$^{-/-}$ mice had only a mild T cell signaling defect. The analysis of *Itk*$^{-/-}$*Rlk*$^{-/-}$ T cells, however, revealed that Rlk can compensate for loss of Itk in TCR-mediated signaling events. Taken together, these studies showed that Itk and Rlk play an important role in the development and function of T cells (for reviews, see Refs. 3–6).

To address the role of Tec in lymphocytes, we analyzed previously generated *Tec*$^{-/-}$ mice (7). Initial studies with *Tec*$^{-/-}$ animals focused on B cells, and it was shown that Tec regulates B cell development in the absence of Btk. With respect to T cells, studies using a murine T cell hybridoma line have shown that Tec is activated in response to TCR/CD28 stimulation (8, 9). CD28 engagement leads to recruitment of Tec to the cytoplasmic tail of CD28, and overexpression of Tec activates both *Il2* and *Il4* promoters (10), However, T cell proliferation and IL-2 production in response to TCR/CD28 stimulation were normal in the absence of Tec (7), although another study showed that downmodulation of Tec kinase by antisense oligonucleotide treatment in primary murine splenocytes impaired *Il2* gene induction (11). Recently, it was reported that Tec expression is upregulated in effector T cells, in particular Th2 cells (12). Taken together, the function of Tec in primary T lymphocytes is poorly understood.

In this study, we performed a comprehensive analysis of the helper T cell lineages in *Tec*$^{-/-}$ mice. *Il23r* and *Rorc* expression were enhanced in CD44^{high}CD62L^{-} *Tec*$^{-/-}$ CD4^{+} T cells, and IL-23–mediated expansion of *Tec*$^{-/-}$ CD4^{+} T cells led to increased production of IL-17. Ex vivo, PMA/ionomycin-stimulated *Tec*$^{-/-}$ splenocytes contained an increased population of IL-17–producing CD44^{high} CD4^{+} T cells, whereas the percentage of IFN-γ– or IL-4–

*Division of Immunobiology, Institute of Immunology, Center for Pathophysiology, Infectiology and Immunology, [†]Center for Molecular Medicine, Austrian Academy of Sciences, [‡]Division of Infectious Diseases and Tropical Medicine, Department of Medicine 1, [¶]Department of Neuroimmunology, Center for Brain Research, and [‖]Division of Immunology, Allergy and Infectious Diseases, Department of Dermatology, Medical University of Vienna, Vienna, Austria; and [§]First Medical Department, Johannes-Gutenberg University of Mainz, Mainz, Germany

[1]Current address: EVER Neuro Pharma, Unterach, Austria.

[2]Current address: Nabriva Therapeutics, Vienna, Austria.

[3]Current address: Institute of Pharmaceutical Sciences, Swiss Federal Institute of Technology Zurich, Zurich, Switzerland.

[4]Current address: Department of Pharmacology and Molecular Sciences, Johns Hopkins University School of Medicine, Baltimore, MD.

Received for publication May 25, 2010. Accepted for publication August 20, 2010.

Work in the laboratory of W.E. was supported by START program (Grant Y-163) of the Austrian Science Fund and the Austrian Ministry of Science and Research, by the Austrian Science Fund (SFB-F2305 and P19930), and by the Vienna Science and Technology Fund (LS09-031). Work in the laboratory of A.W. was funded by the FP6 Marie Curie Research Training Network (MCRTN-CT-2004-005632). U.S. was supported by a postdoctoral fellowship from the Deutsche Forschungsgemeinschaft (Schm 2128/1-1).

Address correspondence and reprint requests to Dr. Wilfried Ellmeier, Division of Immunobiology, Institute of Immunology, Center for Pathophysiology, Infectiology and Immunology, Medical University of Vienna, Lazarettgasse 19, 1090 Vienna, Austria. E-mail address: wilfried.ellmeier@meduniwien.ac.at

The online version of this article contains supplemental material.

Abbreviations used in this paper: AU, arbitrary units; BMDC, bone marrow-derived dendritic cell; con, control; imm, immunized; PLCγ1, phospholipase Cγ1; qRT-PCR, quantitative real-time PCR; rh, recombinant human; *S.p.*, *Streptococcus pneumoniae*.

producing CD44^{high} CD4$^+$ T cells was similar between *Tec*$^{+/+}$ and *Tec*$^{-/-}$ mice. This indicated elevated Th17 effector/memory subsets in Tec-deficient mice. Upon TCR-mediated activation, CD44^{high} CD62L$^-$ *Tec*$^{+/+}$ CD4$^+$ T cells strongly upregulated Tec expression, and CD44^{high}CD62L$^-$ *Tec*$^{-/-}$ CD4$^+$ T cells produced a larger amount of IL-17A (referred to herein as IL-17) and showed increased levels of *Il17f* and *Il21*. Moreover, *Tec*$^{-/-}$ mice immunized with heat-killed *Streptococcus pneumoniae* expressed larger amounts of *Il17* mRNA in the lung after intranasal infection, and this correlated with enhanced pneumococcal clearance and reduced CFU/lung in *Tec*$^{-/-}$ mice. Because IL-17–expressing CD4$^+$ T cells are important for an efficient clearance of *S. pneumoniae* (13, 14), these data suggested increased IL-17–producing CD4$^+$ T cells in Tec-deficient mice upon immunization. Finally, naive *Tec*$^{-/-}$ OT-II CD4$^+$ T cells produced higher levels of IL-17 when stimulated with OVA peptide-loaded bone marrow-derived dendritic cells (BMDCs) that had been previously activated with heat-killed *S. pneumoniae*. Thus, our data suggest a critical role for Tec in T cell-intrinsic signaling pathways that regulate the in vivo generation of a CD44^{high}CD62L$^-$ Th17 effector subset.

Materials and Methods

Mice

Animals used in this study were 6–12 wk of age unless otherwise indicated. The animals were bred and maintained in the animal facility of the Medical University of Vienna, and all animal experiments were approved by the animal committee of the Medical University of Vienna and by Federal Ministry for Science and Research. *Tec*$^{-/-}$ mice were previously described (7) and backcrossed to C57BL/6 for at least 10 generations. OT-II mice (15) expressing a TCR specific for OVA$_{323–339}$ in the context of I-A^b were obtained from Dr. Dagmar Stoiber-Sakaguchi. CD45.1$^+$ congenic mice were obtained from the European Mouse Mutant Archive (Département de Cryopréservation, Distribution, Typage et Archivage Animal, Centre National de la Recherche Scientifique, Orleans, France).

Abs and flow cytometry

The following Abs were used: biotin anti-CD3ε (145-2C11), FITC/TC anti-CD4 (RM4-5), anti-CD16/CD32 (2.4G2), anti-CD28 (37.51), biotin anti-CD45R (B220), FITC anti-CD62L (MEL14), PE anti-CD122 (TM-β1), anti-erythroid cells (Ter-119), unlabeled/FITC anti–IFN-γ (XMG1.2), anti–IL-12 (C17.8), unlabeled/allophycocyanin anti–IL-4 (11B11), PE anti–IL-17 (C17.8), biotin anti–Ly-6G (RB6-8C5), Alexa 647 anti-STAT3 (pY705) (4/P-STAT3), biotin anti-NK1.1 (PK136), and PE anti-γδTCR (GL3) (all from BD Biosciences, San Jose, CA); Pacific Blue anti-CD3ε (500A2), allophycocyanin anti-CD8α (53.6.7), PE-Cy7 anti-CD44 (IM.7.8.1), Alexa 647 anti-FoxP3 (FJK-16s) (all from eBioscience, San Diego, CA); and PE anti-CD25 (PC61.5.3) (Caltag Laboratories, Burlingame, CA). PBS57-loaded and unloaded CD1d tetramers (conjugated with PE) were obtained from the National Institutes of Health Tetramer Facility and used according to the instructions. For flow cytometry, cells were incubated for 30 min at 4°C with the corresponding Abs in 50 μl PBS/2% FBS, followed by two washes in PBS/2% FBS. Samples were acquired on FACSCalibur and LSR II (BD Biosciences) and data were analyzed with FlowJo software (Tree Star, San Carlos, CA).

Purification of CD4$^+$ T cells

Pooled cell suspensions of lymph nodes and spleens were incubated with biotinylated anti- CD8α, anti-CD11b, anti-CD11c, anti-CD45R, anti–Ly-6G, anti–Ter-119, and anti-NK1.1 Abs in PBS/2% FBS. The CD4$^+$ T cells were then purified by negative depletion using streptavidin beads (BD Biosciences) according to the manufacturer's instructions. The purity of the cells was assessed by flow cytometry and was routinely >96%. Where indicated, CD4$^+$ T cells were further sorted into CD44^{low}CD62L$^+$ (naive) and CD44^{high}CD62L$^-$ populations on a FACSAria cytometer (BD Biosciences), and the purity of the populations was routinely >99% for naive cells and >97% for CD44^{high}CD62L$^-$ cells.

T cell proliferation assay

Purified CD4$^+$ T cells (5×10^4 cells/well) were cultured for 72 h in 96-well flat-bottom plates (Nunc, Roskilde, Denmark) coated with anti-CD3ε (0, 0.3, 1, or 10 μg/ml) in a total of 100 μl. Additional wells were coated with anti-CD3ε (1 μg/ml) plus anti-CD28 (3 μg/ml). Forty-four hours later, the cells were pulsed with [^{3}H]thymidine and harvested after 16 h.

Calcium mobilization

T cells (1×10^6/ml) were labeled for 30 min with Fluo3-AM (4 μM) and FuraRed-AM (10 μM) (Molecular Probes, Goettingen, Germany) and the Ca^{2+}-dependent fluorescence was assessed by FACS. Cells were stimulated with soluble bio-anti–CD3ε (1 μg/ml) followed by crosslinking with 5 μg/ml streptavidin (Sigma-Aldrich, St. Louis, MO). Overall Ca^{2+} content was assessed by the addition of ionomycin (1 μM) (Sigma-Aldrich) at the end of each measurement. Data were analyzed using CellQuest (BD Biosciences) and FlowJo (Tree Star) software.

Generation of BMDCs

BMDCs were generated according published protocols (16). Briefly, bone marrow was isolated from tibiae and femurs of 8- to 10-wk-old mice, and single-cell suspensions were cultured at 2×10^6 cells per 100 mm bacteriological Falcon petri dish in 10 ml RPMI GlutaMAX-I (Invitrogen, Carlsbad, CA) supplemented with 10% FCS (Invitrogen), antibiotics, 2-ME (Invitrogen), and 4 ng/ml GM-CSF (PeproTech, Rocky Hill, NJ). Nonadherent cells were fed on days 3, 6 and 9, and BMDCs were harvested on day 10 (~90% were CD11c$^+$). BMDCs were left untreated or were matured and activated for 24 h in the presence of 10^8 heat-inactivated S. *pneumoniae* or 0.1 μg/ml LPS (*Escherichia coli*; Sigma-Aldrich) at 10^6 cells/ml in 24-well cell culture plates (Nunc).

Differentiation of CD4$^+$ T cells and cytokine measurements

Purified CD4$^+$ T cells were stimulated (day 0) with plate-bound anti-CD3ε (1 μg/ml) and anti-CD28 (3 μg/ml) on 48-well plates (0.5×10^6 cells/well for total CD4$^+$ T cells and 1×10^6 cells/well for sorted naive CD4$^+$ T cells) in 1 ml T cell medium (RPMI GlutaMAX-I supplemented with 10% FCS, antibiotics, and 2-ME; all from Invitrogen) under various cytokine conditions. Polarizations were performed as follows: for Th17 conditions, 20 ng/ml IL-6 (R&D Systems, Minneapolis, MN) and 1 ng/ml TGF-β1 (R&D Systems); for inducible regulatory T cell conditions, 1 ng/ml TGF-β1; for IL-23 expansion conditions, 10 ng/ml recombinant murine IL-23 (R&D Systems) plus anti–IFN-γ and anti–IL-4 (10 μg/ml) Abs; for nonpolarizing conditions, recombinant human (rh)IL-2 (20 U/ml); for Th1 conditions, rhIL-2 (20 U/ml), IL-12 (5 ng/ml), and anti–IL-4 (3 μg/ml); for Th2 conditions, IL-4 (250 U/ml), anti–IFN-γ (10 μg/ml), and anti–IL-12 (10 μg/ml). Cells were split 1:2 after 48 h, transferred into new 48-well plates without stimulation, and were further cultured for 2 d (Th17, inducible regulatory T cells) or 3 d (IL-23 expansion, nonpolarizing conditions, Th1, Th2) without addition of additional cytokines (except nonpolarizing conditions, where cultures were supplemented with 20 U/ml rhIL-2) or blocking Abs (except IL-23 expansion cultures, which contained anti–IFN-γ and anti–IL-4 blocking Abs). Th1 and Th2 cultures were further cultured in the presence of rhIL-2 (20 U/ml) and anti–IL-4 (Th1) or anti–IL-12/anti–IFN-γ (Th2). In some experiments, sorted naive CD4$^+$ T cells were also stimulated with anti-CD3ε and anti-CD28 in T cell medium supplemented with supernatant from BMDCs (1:1 [v/v] dilution), which were cultured and activated with heat-killed *S. pneumonia* as described above. T cells were split after 2 d and restimulated on day 4 with anti-CD3ε. IL-17 was determined in supernatants after 12 h by ELISA. For cytokine induction, cells were purified over a Lymphoprep (Cedarlane, Hornby, Ontario, Canada) gradient and restimulated (5×10^5 cells/ml) in 0.2 ml T cell medium with plate-bound anti-CD3ε (0.1 μg/ml) in 96-well plates. Supernatant for cytokine quantification was collected 12 h later.

For the generation of Ag-specific effector CD4$^+$ T cells, 0.5×10^6 naive OT-II CD4$^+$ T cells were cultured with 1×10^5 BMDCs that were either untreated or incubated with heat-inactivated *S. pneumoniae*. BMDCs (1×10^6) were washed in medium and preloaded at 10^6 cells/ml with 5 μM OVA$_{323–339}$ peptide (ISQAVHAAHAEINEAGR) (Anaspec, Fremont, CA) for 30 min at 37°C. Cytokine production was measured in the supernatants after 6 d of culture.

IL-2, IL-4, IL-6, IL-17 IL-23, IFN-γ, and TNF-α cytokine levels were determined by ELISA. The IL-23 ELISA set was from eBioscience, and all others were from BD Biosciences and were used according the manufacturers' protocols. For IL-17 ELISA, capture (anti–IL-17, clone TC11-18H10) and detection (bio-anti–IL-17, clone TC11-8H4.1) Abs were from BD Biosciences. IL-17 standard was from eBioscience. IL-1β, IL-12, and TGF-β1 were determined in supernatants by cytometric bead array from BD Biosciences following the manufacturer's protocol.

Repeated Th17 polarization

Naive CD4$^+$ T cells were stimulated with 1 μg/ml anti-CD3ε and 3 μg/ml anti-CD28 in the presence of 1 ng/ml TGF-β1 and 20 ng/ml IL-6. Cells were split 1:2 after 48 h, transferred into new 48-well plates without stimulation, and were further cultured for 3 d without additional cytokines. On days 5 and 10, the cells were restimulated with 0.3 μg/ml anti-CD3ε in the presence of 1 ng/ml TGF-β1 and 20 ng/ml IL-6 and cultured for another 5 d. IL-17 production on days 5, 10, and 15 was assessed by PMA/ionomycin stimulation in the presence of GolgiStop (BD Biosciences) for 4 h and subsequent intracellular cytokine staining.

Intracellular stainings

Splenocytes, thymocytes, or purified CD4$^+$ T cells that had been cultured under various conditions were stimulated in 6-well plates at 10^6 cells/ml for 4 h with PMA (50 ng/ml) and ionomycin (500 ng/ml) (Sigma-Aldrich) in the presence of GolgiStop). Splenocytes and thymocytes were first incubated with PE-Cy7 anti-CD44, TC-anti-CD4, allophycocyanin-anti-CD8α, and Pacific Blue–anti-CD3ε, or with TC–anti-CD4 only (CD4$^+$ T cell cultures), then fixed with 2% PFA and permeabilized with Perm/Wash solution (BD Pharmingen). Cells were further incubated with FITC-anti–IFN-γ, PE-anti–IL-17, or with allophycocyanin-anti–IL-4 or Alexa 647–anti-FoxP3.

RT-PCR and quantitative real-time PCR analysis

Total RNA was extracted (TRIzol; Sigma-Aldrich) and converted into cDNA using random primers (Fermentas, Burlington, Ontario, Canada) and SuperScript II reverse transcriptase (Invitrogen). cDNA was prepared from in vitro-activated CD4$^+$ T cells after 6 d in culture, restimulated for 8 h with 0.3 μg/ml plate-bound anti-CD3ε, and analyzed by RT-PCR. In addition, samples obtained and treated as indicated in the figure legends were subjected to quantitative real-time PCR (qRT-PCR) analysis on an Applied Biosystems Prism 7300 sequence detection system under standard conditions (Applied Biosystems, Foster City, CA). Genes analyzed were detected using the commercially available SYBR Green assay (Applied Biosystems). *Il23r* mRNA was quantified using a TaqMan gene expression assay (Applied Biosystems), according to the manufacturer's instructions. The following primer sequences were used for RT-PCR and qRT-PCR (designated with an asterisk): *Hprt1* (17), forward, 5′-ATT GTG GCC CTC TGT GTG CT-3′, reverse, 5′-TTG CGC TCA TCT TAG GCT TTG-3′; *Il23r* (18), forward, 5′-TTC TGC GTC CAT CAT TTC CA-3′, reverse, 5′-CCA TTC CCG ACA AAA GTC CA-3′; *Il17f* (18), forward, 5′-CTG GAG GAT AAC ACT GTG AGA GT-3′, reverse, 5′-TGC TGA ATG GCG ACG GAG TTC-3′; *Il17f** (18), forward, 5′-CTG GAG GAT AAC ACT GTG AGA GT-3′, reverse, 5′-TGC TGA ATG GCG ACG GAG TTC-3′; *Il21** (19), forward, 5′-TCA TCA TTG ACC TCG TGG CCC-3′, reverse, 5′-ATC GTA CTT CTC CAC TTG CAA TCC C-3′; *Rorc** (19), forward, 5′-CCG CTG AGA GGG CTT CAC-3′, reverse, 5′-TGC AGG AGT AGG CCA CAT TAC A-3′; *Rlk* (20), forward, 5′-TCA ATC CAA CAG AGG CGG G-3′, reverse, 5′-CCG CTC TCT TCA GTG CCA A-3′; *Itk* (20), forward, 5′-CTC CGC TAT CCA GTT TGC TCC-3′, reverse, 5′-GTC CTT GTT GAG CCA GTA GCC-3′.

Intracellular detection of STAT3 phosphorylation

Sorted naive CD45.1$^+$ wild-type CD4$^+$ T cells were cocultured with either sorted CD45.2$^+$ CD44^{high}CD62L$^-$ *Tec*$^{+/+}$ or *Tec*$^{-/-}$ CD4$^+$ T cells at a ratio that exists in 8-wk-old *Tec*$^{+/+}$ or *Tec*$^{-/-}$ mice (~14:1). Alternatively, CD45.2$^+$ naive *Tec*$^{+/+}$ and *Tec*$^{-/-}$ CD4$^+$ T cells were cocultured with sorted wild-type CD45.1$^+$ CD44^{high}CD62L$^-$ CD4$^+$ T cells. "Mixed" T cell cultures (0.5×10^6 cells/well) were stimulated with plate-bound anti-CD3ε (1 μg/ml) and anti-CD28 (3 μg/ml) on 48-well plates, rested, starved in RPMI 1640 supplemented with 1% FCS for 2 h, and stimulated at 10^7 cells/ml in RPMI 1640/1% FCS with IL-23 (10 ng/ml) or IL-6 (10 ng/ml) for 15 min. Cells were incubated for 20 min in 2% PFA and then 20 min with 80% methanol following the manufacturer's protocol (BD Biosciences). Cells were washed twice with PBS/2% FCS and stained with FITC-anti–CD4, bio-anti–CD45.2, and Alexa 647-anti–p-STAT3 (Y705). Subsequently, cells were washed and then incubated with PE-Cy7-streptavidin. Data were acquired on a FACSCalibur and evaluated using FlowJo software.

Immunoblotting

T cells were pelleted and lysed in Carin lysis buffer (20 mM Tris-HCl [pH 8.0], 138 mM NaCl, 10 mM EDTA, 100 mM NaF, 1% Nonidet P-40, 10% glycerol, 2 mM Na vanadate) supplemented with complete protease inhibitors (Roche, Basel, Switzerland). Proteins were then separated on 10% SDS-polyacrylamide gels and blotted onto polyvinylidene difluoride membranes. For STAT3 immunoblots, cells were purified after 6 d in culture over a Lymphoprep gradient, starved for 1 h in medium containing 1% FCS, and stimulated at 10^7 cells/ml for various time points with IL-23 (10 ng/ml). Anti–p-STAT3 (Y701) Abs were from Cell Signaling Technology (Danvers, MA). The rabbit anti–C-terminal Tec Ab was a gift of H. Mano (Jichi Medical School, Tochigi, Japan). Anti-STAT3 was from Santa Cruz Biotechnology (Santa Cruz, CA). The anti-phosphotyrosine Ab 4G10 was from Upstate Biotechnology (Lake Placid, NY). Secondary Abs were from Jackson ImmunoResearch Laboratories (Suffolk, U.K).

S. pneumoniae *infections*

S. pneumoniae serotype 3 (ATCC 6303) were grown to midlogarithmic phase in Todd-Hewitt broth. Mice were immunized on days 0, 21, and 35

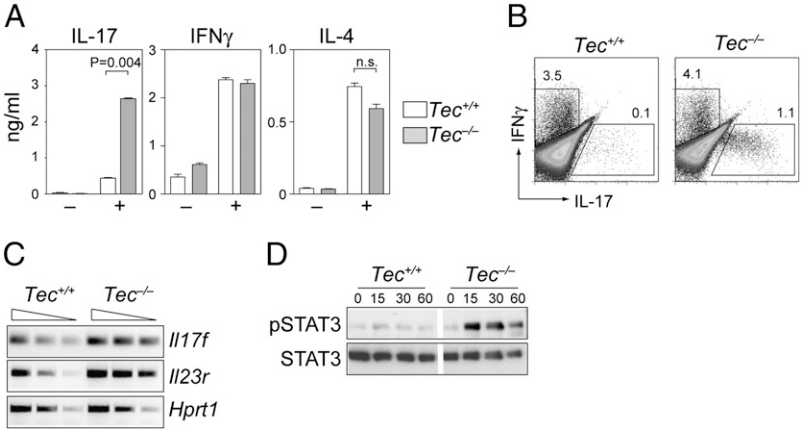

FIGURE 1. Activated *Tec*$^{-/-}$ CD4$^+$ T cells display Th17 features. *A*, IL-17, IFN-γ, and IL-4 expression levels in supernatants of activated total (naive and CD44^{high}) *Tec*$^{+/+}$ and *Tec*$^{-/-}$ CD4$^+$ T cells measured by ELISA. CD4$^+$ T cells were activated with anti-CD3ε plus anti-CD28 in the presence of rhIL-2 and restimulated on day 5 with anti-CD3ε (+). −, Unstimulated controls. Data are representative of five independent experiments. *B*, Intracellular expression of IFN-γ and IL-17 in *Tec*$^{+/+}$ and *Tec*$^{-/-}$ CD4$^+$ T cells cultivated as described in *A*. Cells were restimulated on day 5 with PMA/ionomycin. Data are representative of four independent experiments. *C*, RT-PCR analysis shows *Il17f and Il23r* expression in *Tec*$^{+/+}$ and *Tec*$^{-/-}$ CD4$^+$ T cells cultivated as described in *A* and restimulated with anti-CD3ε. *Hprt1* expression was used as loading control. Data are representative of two independent experiments. *D*, CD4$^+$ T cells were activated as described in *A* and restimulated with IL-23 for the indicated time periods. The phosphorylation status and expression of STAT3 was assessed by immunoblot analysis. Data are representative of three independent experiments. *A–D*, Data shown were generated from the same batch of CD4$^+$ T cells.

with 10^8 heat-killed *S. pneumoniae* in 200 μl PBS i.p. Four weeks later, mice were anesthetized with isoflurane (Baxter, Deerfield, IL), and 8×10^5 CFU *S. pneumoniae* (in 50 μl sterile saline) was inoculated intranasally. Forty-eight hours postinfection, mice were anesthetized with ketamine (Pfizer, New York, NY) and sacrificed by bleeding out via heart puncture. Whole lungs were harvested and homogenized in sterile saline using a tissue homogenizer (Biospec Products, Bartlesville, OK), after which CFU/lung were determined from serial dilutions, plated on blood agar plates, and incubated at 37˚C for 16 h before colonies were counted. Lung homogenate (80 μl) was added to 350 μl RLT buffer (Qiagen, Hilden, Germany) for RNA extraction using a Qiagen RNeasy kit according to the manufacturer's instructions, which included a DNase step.

Histology

Lungs for histology were harvested 48 h after *S. pneumoniae* infection, fixed in 10% formalin, and embedded in paraffin. Four-micrometer sections were stained with H&E and analyzed by a pathologist who was blinded for groups. To score lung inflammation and damage, the entire lung surface was analyzed with respect to the following parameters: interstitial inflammation, edema, endotheliitis, bronchitis, pleuritis, and thrombi formation. Each parameter was graded on a scale of 0–4 as fol lows: 0, absent; 1, mild; 2, moderate; 3, moderately severe; and 4, severe. The inflammation score was expressed as the sum of the scores for each parameter, with the maximum being 24.

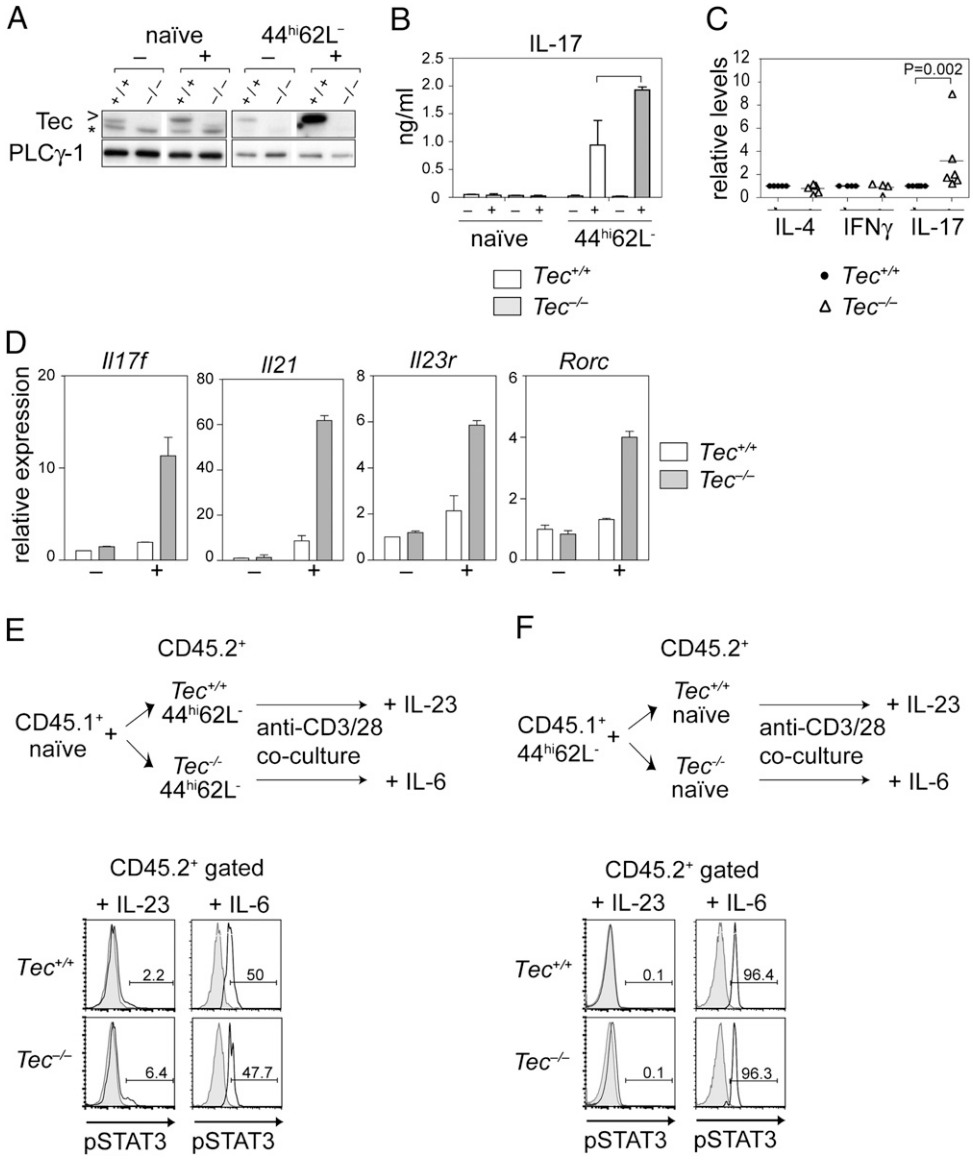

FIGURE 2. Increased Th17 gene expression profile in $Tec^{-/-}$ $CD44^{high}CD62L^{-}$ $CD4^{+}$ T cells upon activation. *A–D*, Naive and $CD44^{high}CD62L^{-}$ $CD4^{+}$ T cells of $Tec^{+/+}$ and $Tec^{-/-}$ mice were activated with anti-CD3ε plus anti-CD28 and restimulated on day 5 with anti-CD3ε. Subsequently, different parameters were investigated without (−) and with (+) anti-CD3ε restimulation. *A*, Expression of Tec was assessed by immunoblot analysis. Phospholipase Cγ1 (PLCγ1) was used as loading control. Data are representative of two independent experiments. *B*, IL-17 secretion was assessed by ELISA. Data are representative of five independent experiments. *C*, Summary showing IL-4, IFN-γ, and IL-17 levels in $CD44^{high}CD62L^{-}$ $CD4^{+}$ T cells as determined by ELISA. For each experiment, $Tec^{+/+}$ cytokine levels were set as one, and the diagram shows relative cytokine levels. Each symbol represents one experiment. *D*, Expression of *Il17f*, *Il21*, *Rorc*, and *Il23r* in $CD44^{high}CD62L^{-}$ $CD4^{+}$ T cells was assessed by qRT-PCR and normalized to *Hprt1* expression. Expression levels in unstimulated $Tec^{+/+}$ $CD44^{high}CD62L^{-}$ $CD4^{+}$ T cells were set as one, and relative expression levels to $Tec^{+/+}$ cells are shown. Data are representative of two independent experiments. *E*, Naive $CD4^{+}$ T cells ($CD45.1^{+}$) were cultured with either $Tec^{+/+}$ or $Tec^{-/-}$ $CD44^{high}CD62L^{-}$ $CD4^{+}$ T cells. The "cocultures" were activated with anti-CD3ε plus anti-CD28 in the presence of rhIL-2. On day 5, cells were restimulated with IL-23 (*left panel*) or IL-6 (*right panel*). The phosphorylation of STAT3 in gated $CD45.2^{+}$ cells was assessed by intracellular pSTAT3 detection. *F*, Naive $Tec^{+/+}$ or $Tec^{-/-}$ $CD4^{+}$ T cells ($CD45.2^{+}$) were cocultured with $CD44^{high}CD62L^{-}$ $CD4^{+}$ T cells ($CD45.1^{+}$) as described in *E*. The cocultures were restimulated on day 5 with IL-23 (*left panel*) or IL-6 (*right panel*). *E* and *F*, Data are representative of two independent experiments. >, Tec-specific band; ∗, nonspecific background band.

Induction of experimental autoimmune encephalomyelitis

Mice were injected s.c. with 100 μl of an emulsion consisting of heat-killed *Mycobacterium tuberculosis*-supplemented (strain H37Ra) CFA (Difco, Detroit, MI) and 50 μg myelin oligodendrocyte glycoprotein peptide (aa 35–55). Mice received 200 ng pertussis toxin (Sigma-Aldrich) i.p. on the day of immunization and 2 d later. Disease progression was assessed daily, and clinical scores were assigned according to the following criteria: 0, unaffected; 1, flaccid tail; 2, impaired righting reflex and/or gait; 3, partial hind limb paralysis; 4, total hind limb paralysis; 5, total hind limb paralysis with partial forelimb paralysis; 6, death.

Induction and evaluation of allergic airway inflammation and mucus production

Mice were immunized with 25 μg OVA (Sigma-Aldrich) or PBS in 2 mg alum i.p. on day 0 and day 5. Mice were challenged 1 wk later with nebulized 1% OVA in PBS with an ultrasonic nebulizer for 60 min twice daily on days 12 and 13. Forty-eight hours after the last aerosol challenge, the tracheas were cannulated and the lungs were lavaged with PBS. Total leukocytes from bronchoalveolar lavage fluid were counted with a hemocytometer. Cytospin slides were stained with May–Grünwald–Giemsa to determine the cell differential.

Statistical analysis

All data are expressed as the mean ± SD (except otherwise indicated). Statistical analysis was performed by using a Student *t* test. The *p* values are indicated in the figures.

Results

Activated $Tec^{-/-}$ $CD4^+$ T cells display Th17 features

Flow cytometric analysis of bone marrow cells or splenocytes for the expression of B220, IgD, IgM, Ter-119, CD61, CD11b, and Gr1 from Tec-deficient mice did not reveal any differences compared with wild-type mice (7). Furthermore, thymocytes and peripheral T cell numbers as well as CD4/CD8 subset distribution are normal in $Tec^{-/-}$ mice (7). Moreover, there was no difference between $Tec^{+/+}$ and $Tec^{-/-}$ $CD4^+$ T cells in the proliferative capacity and production of IL-2 in response to anti-CD3ε with or without anti-CD28 stimulation (Supplemental Fig. 1*A*, 1*B*). Additionally, Ca^{2+} flux and the overall tyrosine phosphorylation patterns were similar in $Tec^{+/+}$ and $Tec^{-/-}$ T cells (Supplemental Fig. 1*C*, 1*D*), indicating normal ex vivo activation upon TCR stimulation. Next, we investigated whether cytokine production is altered upon restimulation of $Tec^{-/-}$ $CD4^+$ T cells. Therefore, purified total $CD4^+$ T cells (i.e., both naive $CD44^{low}CD62L^+$ and $CD44^{high}CD62L^-$ memory-like populations) were activated with anti-CD3ε plus anti-CD28, rested, and restimulated at day 6 with anti-CD3ε. Under these conditions, $Tec^{-/-}$ $CD4^+$ T cells produced much higher levels of IL-17 compared with $Tec^{+/+}$ $CD4^+$ T cells (Fig. 1*A*). In contrast, IL-4 and IFN-γ secretion was not altered in the absence of Tec (Fig. 1*A*). Intracellular cytokine staining of $Tec^{-/-}$ $CD4^+$ T cells revealed the presence of an IL-17–producing subset that was distinct from IFN-γ–producing cells (Fig. 1*B*). Additionally, $Tec^{-/-}$ effector $CD4^+$ T cells expressed also higher levels of other Th17-related genes such as *Il17f* and *Il23r* (for a review, see Ref. 21) upon TCR restimulation (Fig. 1*C*).

IL-23R signaling activates STAT3, and IL-23–activated STAT3 binds to the *Il17* gene locus and induces IL-17 expression (22). Therefore, we investigated whether elevated expression of the *Il23r* in $Tec^{-/-}$ effector $CD4^+$ T cells correlates with increased STAT3 phosphorylation. $Tec^{+/+}$ $CD4^+$ T cells that were previously activated under nonpolarizing conditions showed low levels of STAT3 phosphorylation (pSTAT3) upon IL-23 stimulation, whereas $Tec^{-/-}$ $CD4^+$ T cells displayed much higher levels of pSTAT3 (Fig. 1*D*). These data suggest that increased IL-23R expression in the absence of Tec leads to enhanced pSTAT3 and thus increased IL-17 production upon activation of total $CD4^+$ T cells.

$Tec^{-/-}$ $CD44^{high}CD62L^-$ $CD4^+$ T cells display an enhanced Th17 signature upon TCR stimulation

The IL-23R has been associated with memory $CD44^{high}$ $CD4^+$ T cells (23). To investigate whether the increase in IL-17–producing cells can be directly linked with the $CD44^{high}CD62L^-$ T cell subsets present in the starting cultures of total $CD4^+$ T cells, naive and $CD44^{high}CD62L^-$ $CD4^+$ T cells were sorted and separately analyzed. First, we determined Tec expression levels in naive and $CD44^{high}CD62L^-$ $CD4^+$ T cells, since it was shown that Tec expression in naive $CD4^+$ T cells is upregulated upon activation (12). Tec was strongly upregulated in $CD44^{high}CD62L^-$ $CD4^+$ T cells upon restimulation with anti-CD3ε (Fig. 2*A*),

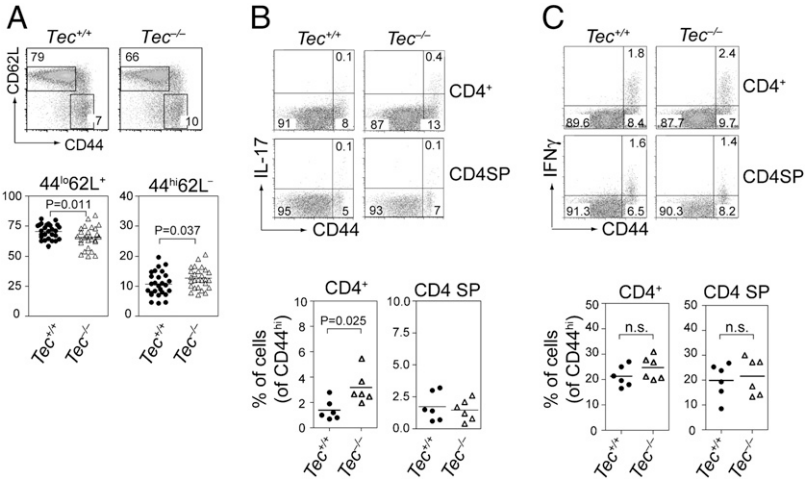

FIGURE 3. Enhanced IL-17 production of $CD44^{high}$ $CD4^+$ T cells upon PMA/ionomycin stimulation. *A*, CD44/CD62L profiles (*upper panel*) of $CD4^+$ T cells from the spleen of $Tec^{+/+}$ and $Tec^{-/-}$ mice. Numbers next to the regions show the percentage of cells. Diagrams (*lower panel*) summarize the percentages of naive ($44^{low}62L^+$) and $CD44^{high}CD62L^-$ ($44^{high}62L^-$) $CD4^+$ T cells from all experiments. Each symbol represents one mouse. *B*, Splenocytes and thymocytes from $Tec^{+/+}$ and $Tec^{-/-}$ mice were stimulated with PMA/ionomycin for 4 h, and IL-17 production was assessed by intracellular cytokine staining. Dot plots show IL-17 versus CD44 expression on gated $CD4^+$ T cells or CD4SP thymocytes. Numbers in each quadrant indicate percentages of each subpopulation. Data are representative of two independent experiments with a total of six mice analyzed. The summary of all experiments is shown in the *lower panel*. *C*, Splenocytes and thymocytes were treated as in *B*, and intracellular IFN-γ expression was determined. The summary of all experiments is shown in the *lower panel*.

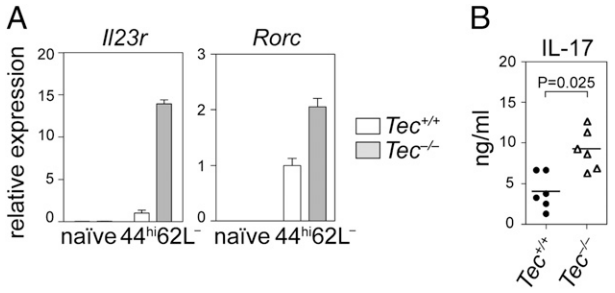

FIGURE 4. CD44^{high}CD62L^{-} CD4^{+} T cells display Th17 features. *A*, Ex vivo expression analysis of *Il23r* and *Rorc* by qRT-PCR in *Tec*$^{+/+}$ and *Tec*$^{-/-}$ CD44^{high}CD62L^{-} CD4^{+} T cells. Expression in each subset was normalized to *Hprt1* expression. For *Il23r* and *Rorc* expression, expression levels in *Tec*$^{+/+}$ CD44^{high}CD62L^{-} CD4^{+} T cells were set as one, and relative expression levels to *Tec*$^{+/+}$ cells are shown. Data are representative of three independent experiments. *B*, Total *Tec*$^{+/+}$ and *Tec*$^{-/-}$ CD4^{+} T cells were stimulated with anti-CD3ε plus anti-CD28 in the presence of IL-23, anti–IL-4, and anti–IFN-γ. Cells were restimulated on day 5 with anti-CD3ε, and IL-17 levels in the supernatant were determined by ELISA. Each symbol represents one mouse.

suggesting an important role of Tec downstream of TCR signaling in this subset. Moreover, *Tec*$^{-/-}$ CD44^{high}CD62L^{-} CD4^{+} T cells that were stimulated with anti-CD3ε plus anti-CD28 and restimulated with anti-CD3ε at day 6 produced higher levels of IL-17 compared with *Tec*$^{+/+}$ CD44^{high}CD62L^{-} CD4^{+} T cells (Fig. 2*B*, 2*C*). The increase in IL-17 was not due to enhanced proliferation, since *Tec*$^{+/+}$ and *Tec*$^{-/-}$ CD4^{+}CD44^{high}CD62L^{-} T cells showed a similar proliferation in response to anti-CD3ε plus anti-CD28 stimulation (data not shown). In contrast, IL-4 and IFN-γ levels were comparable between *Tec*$^{+/+}$ and *Tec*$^{-/-}$ CD44^{high}CD62L^{-} CD4^{+} T cells (Fig. 2*C*). Furthermore, *Tec*$^{-/-}$ CD44^{high}CD62L^{-} CD4^{+} T cells expressed also more *Il17f*, *Il21*, *Il23r*, and *Rorc* (encoding RORγt) (24), the master regulator for Th17 cells (Fig. 2*D*), while *Tbx21* (encoding T-bet) expression was similar between *Tec*$^{+/+}$ and *Tec*$^{-/-}$ CD44^{high}CD62L^{-} CD4^{+} T cells (data not shown). We also observed enhanced STAT3 phosphorylation in *Tec*$^{-/-}$ CD44^{high}CD62L^{-} CD4^{+} T cells compared with *Tec*$^{+/+}$ CD44^{high}CD62L^{-} CD4^{+} T cells upon restimulation with IL-23 (Fig. 2*E*, *left panel*), while restimulation with IL-6, which also signals via STAT3 (25), led to a uniform induction of STAT3 phosphorylation both in naive and in CD44^{high} CD62L^{-} populations of *Tec*$^{+/+}$ and *Tec*$^{-/-}$ CD4^{+} T cells (Fig. 2*E*, 2*F*, *right panels*). These data indicate enhanced Th17 features of CD4^{+} effector T cell subsets in the absence of Tec.

Enhanced Th17 effector subsets in Tec$^{-/-}$ *mice*

Next we wanted to determine whether there is already a difference in IL-17 production between *Tec*$^{+/+}$ and *Tec*$^{-/-}$ naive and CD44^{high}CD62L^{-} CD4^{+} T cells under homeostatic conditions. *Tec*$^{+/+}$ and *Tec*$^{-/-}$ mice displayed a similar CD44/CD62L expression profile on peripheral CD4^{+} T cells, although there was a mild reduction of the naive CD44^{low}CD62L^{+} subsets and a corresponding small increase in CD44^{high}CD62L^{-} effector-like CD4^{+} T cells (Fig. 3*A*). Ex vivo PMA/ionomycin stimulation of splenocytes revealed an increase in IL-17–producing cells within the CD44^{high} CD4^{+} T cells in *Tec*$^{-/-}$ mice (Fig. 3*B*); however, there was no increase in IFN-γ–producing cells within the CD44^{high} subset (Fig. 3*C*). Enhanced IL-17 was also observed when either invariant NKT cells or γδT cells were excluded from the CD4^{+} T cell gate (Supplemental Fig. 2*A*, 2*B*), indicating that the increase in IL-17^{+} cells is not due to differences in innate-like and/or nonconventional T cell subsets. Moreover, the increased IL-17–producing population was only observed in splenic CD4^{+} T cells but not in CD4SP thymocytes from 4- and 8-wk-old mice (Supplemental Fig. 2*C*, Fig. 3*B*, respectively), suggesting that this subset does not represent a distinct helper sublineage that originates already during thymocyte development.

It has been shown that *Il23r* and *Rorc* are expressed ex vivo in CD44^{high}CD62L^{-} CD4^{+} T cells, but not in naive CD4^{+} T cells (23, 24). The observation that *Il23r* and *Rorc* expression is increased upon restimulation in *Tec*$^{-/-}$ CD44^{high}CD62L^{-} CD4^{+} T cells prompted us to test whether in sorted naive and CD44^{high} CD62L^{-} CD4^{+} T cells the *Il23r* and *Rorc* expression differs already between *Tec*$^{+/+}$ and *Tec*$^{-/-}$ mice. Purified *Tec*$^{-/-}$ CD44^{high} CD62L^{-} CD4^{+} T cells displayed increased *Il23r* and *Rorc* ex-

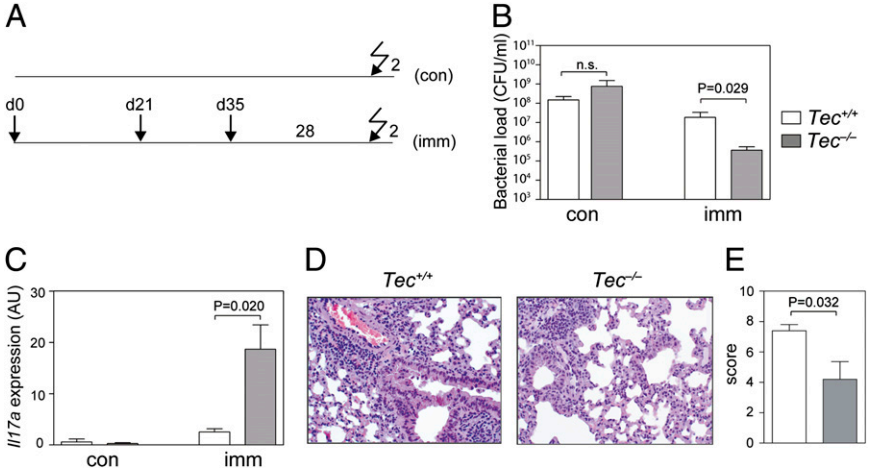

FIGURE 5. Reduced CFU/lung and increased *Il17* expression in the lung of immunized Tec-deficient mice upon *S. pneumoniae* infection. *A*, Treatment scheme of *Tec*$^{+/+}$ and *Tec*$^{-/-}$ mice. Immunizations (i.p.) with heat-killed *S. pneumoniae* were performed at days 0, 21, and 35. Twenty-eight days after the last immunization, mice were infected with *S. pneumoniae* and 2 d later mice were analyzed. Control groups (con) were infected and analyzed without prior immunization. *B*, CFU/lung in control (con) and immunized (imm) *Tec*$^{+/+}$ and *Tec*$^{-/-}$ mice were determined 48 h postinfection. *C*, Expression of *Il17a* in the lung of infected *Tec*$^{+/+}$ and *Tec*$^{-/-}$ mice was assessed by qRT-PCR and normalized to *Hprt1* expression. Expression levels are shown in arbitrary units (AU). Data show summary of two independent experiments performed in duplicates. *D*, Images show representative photomicrographs of H&E-stained lung tissue sections of immunized *Tec*$^{+/+}$ and *Tec*$^{-/-}$ mice 48 h postinfection (original magnification ×10). *E*, Lung slides were scored for the presence of inflammation as described in *Materials and Methods*. Data represent mean ± SEM. *A–E*, Data are representative of five mice/group.

pression levels compared with *Tec*$^{+/+}$ CD44^{high}CD62L^{-} CD4^{+} T cells, whereas *Il23r* and *Rorc* expression was not detectable in the naive subsets of both genotypes (Fig. 4*A*).

IL-23 promotes the expansion and survival of already existing Th17 effector/memory cells (23, 25–28). To test whether IL-23–mediated expansion of Th17 cells is altered in the absence of Tec, *Tec*$^{+/+}$ and *Tec*$^{-/-}$ CD4^{+} T cells were stimulated in the presence of IL-23 and anti–IFN-γ and anti–IL-4 Abs. Under these conditions, *Tec*$^{-/-}$ CD4^{+} T cells produced enhanced levels of IL-17 compared with their *Tec*$^{+/+}$ counterparts (Fig. 4*B*). Thus, increased *Il23r* and *Rorc* expression in *Tec*$^{-/-}$ CD44^{high}CD62L^{-} CD4^{+} T cells is linked with enhanced production of IL-17 in IL-23–mediated expansion cultures or in stimulated splenocytes.

Tec-deficient mice immunized with heat-killed S. pneumoniae *display enhanced pneumococcal clearance postinfection*

Th17 cells are important for an efficient clearance of *S. pneumoniae* colonization in the lung (13, 14). To investigate whether the increased IL-17–producing CD4^{+} T cell population with a Th17 signature in *Tec*$^{-/-}$ mice leads to a better protection against *S. pneumoniae*, *Tec*$^{+/+}$ and *Tec*$^{-/-}$ mice were intranasally infected and CFU/lung and lung IL-17 expression were determined 48 h postinfection (Fig. 5*A*). Under these conditions, similar CFU/lung were detected in *Tec*$^{+/+}$ and *Tec*$^{-/-}$ mice (Fig. 5*B*) and there was no difference in the expression of IL-17 (Fig. 5*C*). To study whether *S. pneumoniae*-specific effector/memory Th17 responses in *Tec*$^{-/-}$ mice are enhanced, *Tec*$^{+/+}$ and *Tec*$^{-/-}$ mice were immunized i.p. with heat-killed *S. pneumoniae* followed by two booster injections at days 21 and 35. Twenty-eight days after the last injection, mice were infected intranasally and CFU/lung were determined 2 d postinfection (Fig. 5*A*). *Tec*$^{-/-}$ mice showed decreased levels of CFU/lung compared with immunized *Tec*$^{+/+}$ mice (Fig. 5*B*), as well as reduced signs of inflammation (Fig. 5*D*, 5*E*), indicating a better bacterial clearance in the lung. The enhanced clearance of *S. pneumoniae* correlated with increased *Il17* expression levels in *Tec*$^{-/-}$ lung homogenates (Fig. 5*C*).

T cell-intrinsic alterations in the absence of Tec

Since Tec-deficient CD44^{+}CD62L^{-} CD4^{+} T cells produced enhanced levels of IL-17, we tested whether the in vitro generation of Th17 cells is altered in the absence of Tec. Th17 cells generated from naive *Tec*$^{-/-}$ CD4^{+} T cells in the presence of TGF-β1 plus IL-6 (27) produced similar levels of IL-17 compared with *Tec*$^{+/+}$ cells (Fig. 6*A*, *upper panels*, and Fig. 6*B*), indicating that Tec kinase does not regulate the in vitro differentiation of Th17 cells via TGF-β1 and IL-6. Tec was also not required for the development of FoxP3-expressing inducible regulatory T cells generated from naive CD4^{+} T cells in the presence of TGF-β1 (Fig. 6*A*, *lower panels*).

Because immunization with heat-killed *S. pneumoniae* prior to infection resulted in enhanced *Il17* expression in the lung of *Tec*$^{-/-}$ mice, we tested whether naive *Tec*$^{-/-}$ CD4^{+} T cells might show enhanced IL-17 production if stimulated with dendritic cells that have been activated with heat-killed *S. pneumoniae*. For this, *Tec*$^{+/+}$ and *Tec*$^{-/-}$ mice were intercrossed with OT-II transgenic mice, which express TCRs ($V_{\beta}5$, $V_{\alpha}2$) restricted to MHC class II. Naive *Tec*$^{+/+}$ and *Tec*$^{-/-}$ OT-II CD4^{+} T cells were isolated and incubated with OVA peptide-loaded *Tec*$^{+/+}$ or *Tec*$^{-/-}$ BMDCs that have been previously activated with heat-killed *S. pneumoniae*. *Tec*$^{-/-}$ OT-II CD4^{+} T cells showed enhanced IL-17 production compared with *Tec*$^{+/+}$ OT-II CD4^{+} T cells when incubated with heat-killed *S. pneumoniae*-activated *Tec*$^{+/+}$ BMDCs (Fig. 6*C*). A similar increase in IL-17 production was also observed when naive *Tec*$^{-/-}$ OT-II CD4^{+} T cells were stimulated with OVA peptide-loaded *Tec*$^{-/-}$ BMDCs that have been previously activated with heat-killed *S. pneumoniae* (Fig. 6*C*). Taken together, these data strongly suggest a T cell-intrinsic defect in the absence of Tec.

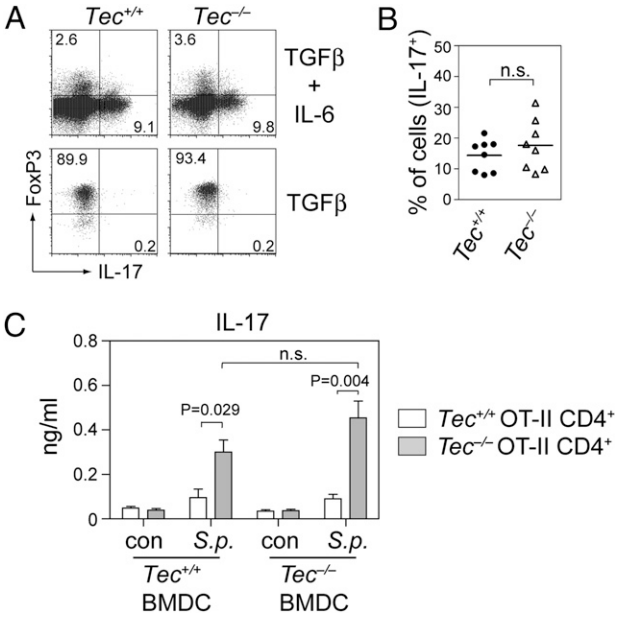

FIGURE 6. Ag-specific activation reveals T cell-intrinsic defects in Tec-deficient CD4^{+} T cells. *A*, *Tec*$^{+/+}$ and *Tec*$^{-/-}$ naive CD4^{+} T cells were stimulated under Th17 or inducible regulatory T cell conditions. Cells were restimulated on day 4 with PMA/ionomycin. Intracellular expression of IL-17 and FoxP3 in *Tec*$^{+/+}$ and *Tec*$^{-/-}$ Th17 (*upper panel*) and regulatory T (*lower panel*) cells is differentiated from naive CD4^{+} T cells. Numbers in the dot plots indicate the percentage of cells in the respective quadrants. Data shown are representative of eight independent experiments for TGF-β1 plus IL-6 Th17 differentiation cultures, and of two independent experiments for TGF-β1–induced regulatory T cell differentiation. *B*, Diagram represents the summary of all Th17 differentiations as described in *A*. *C*, Naive *Tec*$^{+/+}$ and *Tec*$^{-/-}$ OT-II CD4^{+} T cells were isolated and incubated for 5 d with OVA peptide-loaded *Tec*$^{+/+}$ or *Tec*$^{-/-}$ BMDCs that have been previously activated with heat-killed *S. pneumoniae* (*S.p.*) or that have not been activated (con). IL-17 cytokine levels in the supernatants of the T/DC cocultures were determined by ELISA. Data show the summary of three independent experiments.

Discussion

In this study, we investigated the role of the nonreceptor protein tyrosine kinase Tec in CD4^{+} helper T cells. Our study revealed that Tec had no major role during T cell development and for anti-CD3ε with or without anti-CD28–induced proliferation. Although studies suggested that Tec is involved in the activation of the IL-4 promoter (10) and that Tec is upregulated in Th2 cells (12), we did not observe any alteration in the Th2 (or in Th1) cytokine pattern of *Tec*$^{-/-}$ CD4^{+} T cells in vitro (Supplemental Fig. 3). Moreover, there was a similar eosinophil infiltration in the lung of *Tec*$^{+/+}$ and *Tec*$^{-/-}$ mice in a Th2-driven allergic airway inflammation model (Supplemental Fig. 4). This is in contrast to Itk, which plays an important role in these processes (4, 5). This indicates a different utilization of Tec family kinases in the T cell lineage. Whether other Tec family kinases compensate for the loss of Tec in Th2-dependent processes remains to be determined; however, there was no compensatory upregulation of Itk or Rlk in the absence of Tec under homeostatic conditions (Supplemental Fig. 5).

An important finding of our study is the identification of an essential role for Tec in the regulation of a CD44^{high}CD62L^{-} Th17 subset. CD44^{high}CD62L^{-} CD4^{+} T cells are slightly increased in Tec-deficient mice, and they produced more IL-17 upon

activation compared with $Tec^{+/+}$ mice. Because Th1 or Th2 memory cells were not increased, this indicated a general bias toward a Th17 memory in $Tec^{-/-}$ mice. We consider it unlikely that this $CD44^{high}$ subset represents an innate-like lineage with immediate effector function similar to the increase in innate-like T cells observed in Itk-deficient mice (29–33) or that a natural Th17 population as described recently (34) was expanded in the absence of Tec. The increase in IL-17–producing $CD44^{high}$ $CD4^+$ T cells upon PMA/ionomycin stimulation was restricted to peripheral $CD4^+$ T cells and not observed in CD4SP thymocytes. This argues against a distinct lineage already generated in the thymus. Also, we did not observe alterations in invariant NKT and γδT cell subsets. Thus, our results rather indicate that conventional Th17 subsets are enhanced in $Tec^{-/-}$ mice and that TCR stimulation leads to an expansion of these Th17 effector/memory subsets. First, we observed that ex vivo-isolated $CD44^{high}CD62L^-$ $CD4^+$ T cells expressed increased levels of *Il23r* and *Rorc* in the absence of Tec. Second, the addition of IL-23, known to induce the expansion of preformed effector Th17 cells (23, 27, 28, 35), led to increased IL-17 levels in $Tec^{-/-}$ $CD4^+$ T cell cultures. Third, upon activation, $Tec^{-/-}$ $CD44^{high}CD62L^-$ $CD4^+$ T cells expressed also higher levels of *Il17f* and *Il21*, which is indicative of a Th17 signature. Additionally, lungs of $Tec^{-/-}$ mice displayed reduced inflammation and enhanced IL-17 expression compared with $Tec^{+/+}$ mice after *S. pneumoniae* infection, but only if mice were immunized with heat-killed *S. pneumoniae* before the infection. This suggests that there might be also enhanced Th17 memory development in Tec-deficient mice during an immune response, leading to a protective Th17 response upon rechallenge. Taken together, these data indicate that Tec deficiency enhances the in vivo generation of a $CD44^{high}CD62L^-$ Th17 effector/memory subset.

One question that arises is why a $CD44^{high}CD62L^-$ $CD4^+$ T cells subset with Th17 characteristics is enhanced in the absence of Tec. In vitro, Th17 differentiation from naive $CD4^+$ T cells was shown to occur upon anti-CD3ε/CD28 stimulation in the presence of IL-6 plus TGF-β1 (27); however, other cytokines were shown to contribute to the differentiation and homeostatic maintenance of Th17 cells (19, 36, 37). $Tec^{-/-}$ Th17 cells (as well as transgenic OT-II $Tec^{-/-}$ Th17 cells; data not shown) generated with IL-6 plus TGF-β1 did not display differences in the extent of IL-17 production even after repetitive stimulation (Supplemental Fig. 6). However, naive $Tec^{-/-}$ OT-II $CD4^+$ T cells produced more IL-17 compared with $Tec^{+/+}$ OT-II $CD4^+$ T cells when stimulated with OVA peptide-loaded BMDCs that were matured/activated with heat-killed *S. pneumoniae*, an extracellular bacterium that elicits Th17 responses in vivo (13, 14). This indicates that naive $Tec^{-/-}$ $CD4^+$ T cells, dependent on the activation conditions, have the potential to produce more IL-17 than do their $Tec^{+/+}$ counterparts. Moreover, this suggests that the increase in Th17 effector T cells in vivo might be in part due to T cell-intrinsic defects. The strong upregulation of Tec expression in activated $CD44^{high}$ $CD4^+$ T cells further suggests a T cell-intrinsic role for Tec downstream of TCR signaling. However, preliminary results showed that $Tec^{-/-}$ BMDCs produced increased levels of TGF-β1 even without activation, and after activation with heat-killed *S. pneumoniae* they also produced increased levels of IL-6, IL-1β, IL-23, and TNF-α, all cytokines that favor Th17 responses (Supplemental Fig. 7*A*). Moreover, supernatants from heat-killed *S. pneumoniae*-treated $Tec^{-/-}$ BMDCs induced more IL-17 production in wild-type T cells compared with $Tec^{+/+}$ BMDC supernatants (Supplemental Fig. 7*B*). It is therefore likely that T cell-intrinsic alterations together with T cell-extrinsic changes lead to the enhanced Th17 $CD44^{high}CD62L^-$ subset in $Tec^{-/-}$ mice, and that the enhanced Th17 subsets under homeostatic conditions might have arisen from an altered response against commensal bacteria in the absence of Tec (21, 38).

$Tec^{-/-}$ $CD44^{high}CD62L^-$ $CD4^+$ T cells expressed higher amounts of *Il17a* and *Il17f*. Thus, the role of Tec in Th17 cells is different to the function of Itk. Whereas Itk selectively regulates the expression of *Il17a* but not of *Il17f* in an NFAT-dependent manner (39), Tec negatively regulates Th17 signature genes such as *Il17a*, *Il17f*, *Rorc*, *Il21*, and *Il23r*. However, $Tec^{-/-}$ mice showed a similar incidence and clinical score compared with $Tec^{+/+}$ mice in an experimental autoimmune encephalomyelitis model (Supplemental Fig. 8). In contrast, Tec-deficient mice displayed enhanced pneumococcal clearance and IL-17 expression in the lung after immunization and infection. Since IL-17 production is beneficial for immunity against a growing number of extracellular pathogens, including *S. pneumoniae* (13, 14, 40), it is tempting to speculate that Tec might be a potential target to increase host defense against these pathogens without raising the risk for Th17-mediated autoimmunity.

Taken together, our study showed that Tec deficiency leads to the enhanced in vivo generation of Th17 effector/memory subsets. Additional studies aiming to further characterize the cellular and molecular pathways controlled by Tec in $CD4^+$ T cells and other hematopoietic cells are required to fully understand the role of Tec in the generation and function of Th17 cells.

Acknowledgments

We thank Drs. Thomas Wekerle and Shinya Sakaguchi for critical reading of the manuscript.

Disclosures

The authors have no financial conflicts of interest.

References

1. Blomberg, K. E., C. I. Smith, and J. M. Lindvall. 2007. Gene expression signatures in primary immunodeficiencies: the experience from human disease and mouse models. *Curr. Mol. Med.* 7: 555–566.
2. Huck, K., O. Feyen, T. Niehues, F. Rüschendorf, N. Hübner, H. J. Laws, T. Telieps, S. Knapp, H. H. Wacker, A. Meindl, et al. 2009. Girls homozygous for an IL-2-inducible T cell kinase mutation that leads to protein deficiency develop fatal EBV-associated lymphoproliferation. *J. Clin. Invest.* 119: 1350–1358.
3. Berg, L. J. 2007. Signalling through TEC kinases regulates conventional versus innate $CD8^+$ T-cell development. *Nat. Rev. Immunol.* 7: 479–485.
4. Readinger, J. A., K. L. Mueller, A. M. Venegas, R. Horai, and P. L. Schwartzberg. 2009. Tec kinases regulate T-lymphocyte development and function: new insights into the roles of Itk and Rlk/Txk. *Immunol. Rev.* 228: 93–114.
5. Prince, A. L., C. C. Yin, M. E. Enos, M. Felices, and L. J. Berg. 2009. The Tec kinases Itk and Rlk regulate conventional versus innate T-cell development. *Immunol. Rev.* 228: 115–131.
6. Lindvall, J. M., K. E. Blomberg, J. Väliaho, L. Vargas, J. E. Heinonen, A. Berglöf, A. J. Mohamed, B. F. Nore, M. Vihinen, and C. I. Smith. 2005. Bruton's tyrosine kinase: cell biology, sequence conservation, mutation spectrum, siRNA modifications, and expression profiling. *Immunol. Rev.* 203: 200–215.
7. Ellmeier, W., S. Jung, M. J. Sunshine, F. Hatam, Y. Xu, D. Baltimore, H. Mano, and D. R. Littman. 2000. Severe B cell deficiency in mice lacking the tec kinase family members Tec and Btk. *J. Exp. Med.* 192: 1611–1624.
8. Yang, W. C., M. Ghiotto, B. Barbarat, and D. Olive. 1999. The role of Tec protein-tyrosine kinase in T cell signaling. *J. Biol. Chem.* 274: 607–617.
9. Garçon, F., M. Ghiotto, A. Gérard, W. C. Yang, D. Olive, and J. A. Nunès. 2004. The SH3 domain of Tec kinase is essential for its targeting to activated CD28 costimulatory molecule. *Eur. J. Immunol.* 34: 1972–1980.
10. Yang, W. C., and D. Olive. 1999. Tec kinase is involved in transcriptional regulation of IL-2 and IL-4 in the CD28 pathway. *Eur. J. Immunol.* 29: 1842–1849.
11. Yang, W. C., K. A. Ching, C. D. Tsoukas, and L. J. Berg. 2001. Tec kinase signaling in T cells is regulated by phosphatidylinositol 3-kinase and the Tec pleckstrin homology domain. *J. Immunol.* 166: 387–395.
12. Tomlinson, M. G., L. P. Kane, J. Su, T. A. Kadlecek, M. N. Mollenauer, and A. Weiss. 2004. Expression and function of Tec, Itk, and Btk in lymphocytes: evidence for a unique role for Tec. *Mol. Cell. Biol.* 24: 2455–2466.
13. Zhang, Z., T. B. Clarke, and J. N. Weiser. 2009. Cellular effectors mediating Th17-dependent clearance of pneumococcal colonization in mice. *J. Clin. Invest.* 119: 1899–1909.
14. Lu, Y. J., J. Gross, D. Bogaert, A. Finn, L. Bagrade, Q. Zhang, J. K. Kolls, A. Srivastava, A. Lundgren, S. Forte, et al. 2008. Interleukin-17A mediates acquired immunity to pneumococcal colonization. *PLoS Pathog.* 4: e1000159.

15. Barnden, M. J., J. Allison, W. R. Heath, and F. R. Carbone. 1998. Defective TCR expression in transgenic mice constructed using cDNA-based α- and β-chain genes under the control of heterologous regulatory elements. *Immunol. Cell Biol.* 76: 34–40.
16. Lutz, M. B., N. Kukutsch, A. L. Ogilvie, S. Rössner, F. Koch, N. Romani, and G. Schuler. 1999. An advanced culture method for generating large quantities of highly pure dendritic cells from mouse bone marrow. *J. Immunol. Methods* 223: 77–92.
17. Bilic, I., C. Koesters, B. Unger, M. Sekimata, A. Hertweck, R. Maschek, C. B. Wilson, and W. Ellmeier. 2006. Negative regulation of CD8 expression via *Cd8* enhancer-mediated recruitment of the zinc finger protein MAZR. *Nat. Immunol.* 7: 392–400.
18. Yang, X. O., A. D. Panopoulos, R. Nurieva, S. H. Chang, D. Wang, S. S. Watowich, and C. Dong. 2007. STAT3 regulates cytokine-mediated generation of inflammatory helper T cells. *J. Biol. Chem.* 282: 9358–9363.
19. Nurieva, R., X. O. Yang, G. Martinez, Y. Zhang, A. D. Panopoulos, L. Ma, K. Schluns, Q. Tian, S. S. Watowich, A. M. Jetten, and C. Dong. 2007. Essential autocrine regulation by IL-21 in the generation of inflammatory T cells. *Nature* 448: 480–483.
20. Lucas, J. A., M. Felices, J. W. Evans, and L. J. Berg. 2007. Subtle defects in pre-TCR signaling in the absence of the Tec kinase Itk. *J. Immunol.* 179: 7561–7567.
21. Littman, D. R., and A. Y. Rudensky. 2010. Th17 and regulatory T cells in mediating and restraining inflammation. *Cell* 140: 845–858.
22. Chen, Z., A. Laurence, and J. J. O'Shea. 2007. Signal transduction pathways and transcriptional regulation in the control of Th17 differentiation. *Semin. Immunol.* 19: 400–408.
23. Aggarwal, S., N. Ghilardi, M. H. Xie, F. J. de Sauvage, and A. L. Gurney. 2003. Interleukin-23 promotes a distinct CD4 T cell activation state characterized by the production of interleukin-17. *J. Biol. Chem.* 278: 1910–1914.
24. Ivanov, I. I., B. S. McKenzie, L. Zhou, C. E. Tadokoro, A. Lepelley, J. J. Lafaille, D. J. Cua, and D. R. Littman. 2006. The orphan nuclear receptor RORγt directs the differentiation program of proinflammatory IL-17$^+$ T helper cells. *Cell* 126: 1121–1133.
25. Zhou, L., I. I. Ivanov, R. Spolski, R. Min, K. Shenderov, T. Egawa, D. E. Levy, W. J. Leonard, and D. R. Littman. 2007. IL-6 programs T_H-17 cell differentiation by promoting sequential engagement of the IL-21 and IL-23 pathways. *Nat. Immunol.* 8: 967–974.
26. Frucht, D. M. 2002. IL-23: a cytokine that acts on memory T cells. *Sci. STKE* 2002: pe1.
27. Veldhoen, M., R. J. Hocking, C. J. Atkins, R. M. Locksley, and B. Stockinger. 2006. TGFβ in the context of an inflammatory cytokine milieu supports de novo differentiation of IL-17-producing T cells. *Immunity* 24: 179–189.
28. Stritesky, G. L., N. Yeh, and M. H. Kaplan. 2008. IL-23 promotes maintenance but not commitment to the Th17 lineage. *J. Immunol.* 181: 5948–5955.
29. Atherly, L. O., J. A. Lucas, M. Felices, C. C. Yin, S. L. Reiner, and L. J. Berg. 2006. The Tec family tyrosine kinases Itk and Rlk regulate the development of conventional CD8$^+$ T cells. *Immunity* 25: 79–91.
30. Broussard, C., C. Fleischacker, R. Horai, M. Chetana, A. M. Venegas, L. L. Sharp, S. M. Hedrick, B. J. Fowlkes, and P. L. Schwartzberg. 2006. Altered development of CD8$^+$ T cell lineages in mice deficient for the Tec kinases Itk and Rlk. *Immunity* 25: 93–104.
31. Dubois, S., T. A. Waldmann, and J. R. Müller. 2006. ITK and IL-15 support two distinct subsets of CD8$^+$ T cells. *Proc. Natl. Acad. Sci. USA* 103: 12075–12080.
32. Hu, J., N. Sahu, E. Walsh, and A. August. 2007. Memory phenotype CD8$^+$ T cells with innate function selectively develop in the absence of active Itk. *Eur. J. Immunol.* 37: 2892–2899.
33. Hu, J., and A. August. 2008. Naive and innate memory phenotype CD4$^+$ T cells have different requirements for active Itk for their development. *J. Immunol.* 180: 6544–6552.
34. Marks, B. R., H. N. Nowyhed, J. Y. Choi, A. C. Poholek, J. M. Odegard, R. A. Flavell, and J. Craft. 2009. Thymic self-reactivity selects natural interleukin 17-producing T cells that can regulate peripheral inflammation. *Nat. Immunol.* 10: 1125–1132.
35. Chen, Z., A. Laurence, Y. Kanno, M. Pacher-Zavisin, B. M. Zhu, C. Tato, A. Yoshimura, L. Hennighausen, and J. J. O'Shea. 2006. Selective regulatory function of Socs3 in the formation of IL-17-secreting T cells. *Proc. Natl. Acad. Sci. USA* 103: 8137–8142.
36. Chung, Y., S. H. Chang, G. J. Martinez, X. O. Yang, R. Nurieva, H. S. Kang, L. Ma, S. S. Watowich, A. M. Jetten, Q. Tian, and C. Dong. 2009. Critical regulation of early Th17 cell differentiation by interleukin-1 signaling. *Immunity* 30: 576–587.
37. Korn, T., E. Bettelli, W. Gao, A. Awasthi, A. Jäger, T. B. Strom, M. Oukka, and V. K. Kuchroo. 2007. IL-21 initiates an alternative pathway to induce proinflammatory T_H17 cells. *Nature* 448: 484–487.
38. Surh, C. D., O. Boyman, J. F. Purton, and J. Sprent. 2006. Homeostasis of memory T cells. *Immunol. Rev.* 211: 154–163.
39. Gomez-Rodriguez, J., N. Sahu, R. Handon, T. S. Davidson, S. M. Anderson, M. R. Kirby, A. August, and P. L. Schwartzberg. 2009. Differential expression of interleukin-17A and -17F is coupled to T cell receptor signaling via inducible T cell kinase. *Immunity* 31: 587–597.
40. Curtis, M. M., and S. S. Way. 2009. Interleukin-17 in host defence against bacterial, mycobacterial and fungal pathogens. *Immunology* 126: 177–185.